# ENHANCED PERFORMANCE OF DSSCs USING Ag-DOPED ZnO THIN FILMS SYNTHESIZED BY SUCCESSIVE IONIC LAYER ADSORPTION AND REACTION METHOD

Mangesh K. Lanjewar[1], Jignasa V. Gohel[2]

[1]*Department of Chemical Engineering, Government Engineering College Bharuch, Gujarat, India 392001, mangesh.lanjewar@gmail.com (M.K.L)*
[2]*Department of Chemical Engineering Sardar Vallabhbhai National Institute of Technology Surat 395007, Gujarat, India 395007, sjn@ched.svnit.ac.in (J.V.G)*

*Received 12 May 2025*
*Accepted 29 July 2025*
*DOI: 10.59957/jctm.v61.i2.2026.5*

## ABSTRACT

*Pure ZnO thin films and Ag doped ZnO (Ag:ZnO) thin films are successfully synthesized using low-cost method. SILAR (Successive Ionic layer Adsorption and reaction) technique is also very easy and simple. The dopant amount is further optimized by varying Ag percentages and investing corresponding optical properties. For 6 wt. % Ag:ZnO, maximum red shift is observed (from 372 to 400 nm). Band gap is also observed to be altered with maximum reduction achieved for 6 wt. % Ag:ZnO thin film (from 2.99 eV for pure ZnO to 2.7 eV). Consequently, optimum (6 wt. %) Ag:ZnO thin film is further used as photoanode in dye sensitized solar cell (DSSC). Additionally, low-cost dye is used in place of expensive dyes used generally in DSSCs. Further structural and morphological characterization of optimum (6 wt. %) Ag:ZnO thin film is also carried over by X-ray diffraction (XRD) and scanning electron microscopy (SEM). Prepared films are observed to be polycrystalline and hexagonal in structure. DSSC made of Ag:ZnO thin film along with inexpensive dye could yet lead to reasonable conversion efficiency. Furthermore, reasonable increment in efficiency (50 %) is achieved compared to DSSC made with pure ZnO film.*

*Keywords: Ag doped ZnO, low-cost dye, dye sensitized solar cell, SILAR method.*

## INTRODUCTION

Dye-sensitized solar cell (DSSC) has gained a lot of interest in recent time due to prospective applications in various solar cells and low cost [1 - 3]. However, efficiency of DSSCs depends on electrical and optical properties of photoanode. Due to its outstanding properties, semiconductor oxide thin films are potential candidate for photoanode preparation [4]. However, most of the research work on DSSC is mainly focused on $TiO_2$ based thin films.

On the other hand, ZnO based thin films have higher electron mobility than $TiO_2$and other semiconductors [8]. Additionally, ZnO thin films have enhanced properties including stability [5], radiation hardness, biocompatibility [6] and elevated optical transparency [7]. Hence, ZnO is gaining research interests in recent time. It is recently reported in the areas of application including, dye-sensitized solar cell [8], gas sensor [9], antireflection coating [10], transparent conducting material [5] photoelectrochemical cell [11], and photo catalysis [12] etc. Thus, in the present work, we have attempted to achieve ZnO based thin films in DSSC.

Basically, ZnO is a semiconductor having the wide band gap (3.2 - 3.37 eV) at room temperature [12], so it can absorb mainly UV light spectrum (due to high energy of UV light) from the solar light spectrum. However, upon doping by metals or non-metals, it can also absorb the visible light spectrum in addition to UV range. As visible spectrum possesses a considerable part of the solar spectrum, its absorption will lead to enhanced efficiency.

In addition, upon doping, other properties of ZnO thin films are also enhanced [13]. Doping of ZnO is

reported in the literature with various dopants, such as, copper (Cu), manganese (Mn), indium (In), aluminium (Al), gallium (Ga), and nickel (Ni) [13 - 16].

Ag can be a remarkable dopant, because it possesses high photocatalytic activity, antibacterial activity [17], and luminescent properties [18]. Consequently, Ag doped ZnO will lead to highly active photocatalytic thin film. However, to our best knowledge, Ag doped ZnO films have been scarcely used in DSSCs till date [19]. In addition, most of the reports in literature on ZnO thin film preparation represents the use of various methods including sputtering [5, 12], chemical vapor deposition (CVD) [20], physical vapor deposition [21], spray pyrolysis [11], and sol gel spin coating [22, 23]. Nevertheless, the above techniques require high temperature, high pressure, and high cost. In our previous work, thin films and nanomaterials are prepared with the soft and low-cost techniques, such as, sol-gel method, microemulsion and colloidal techniques [19, 22 - 27]. In particular, the low-cost DSSC prepared (in our previous work) is first time reported with the doped Ag:ZnO films (with sol gel spin-coating method) [19, 28]. In addition, Ag:ZnO films prepared in our recent studies also confirmed superior performance [29, 30].

In continuation to this, a low-cost method (SILAR) is explored in the present study for DSSC preparation with doped Ag:ZnO films. Because, SILAR method possesses many advantages, such as, (i) it is simple and economic [4], (ii) it is convenient for large scale production [4], (iii) it can operate at ambient temperature and pressure, and (iv) it gives superior control of deposition rate and thickness of film (by optimizing the dipping time and number of cycles) [4]. As per our best knowledge, Ag doped ZnO thin film preparation by SILAR method is not reported yet. In addition, N719 and N3 types of dyes are used generally for sensitization of solar cell. However, these dyes are very costly. Therefore, the cost of solar cell is increased. There is a need to use alternative economic dyes, e.g. mercurochrome.

Hence, in the present work, we have successfully attempted to prepare very low-cost DSSC by using Ag:ZnO thin films prepared by SILAR technique and using a low-cost dye as well. The weight percentage of Ag (as dopant on ZnO) is varied from 2 - 10 wt. % and spectroscopy analysis was performed to find optical wt. %. Band gap is also obtained. Optimum doping percentage is identified and the same is further used for DSSC application. Structural properties of the optimum doped ZnO thin film is further investigated by X-ray diffraction (XRD). Surface analysis was performed by scanning electron microscopy (SEM). Furthermore, use of an economic dye (mercurochrome) in DSSC application is investigated by I-V characteristics. A reasonable improvement in efficiency is obtained for doped ZnO thin films despite using a cheap dye.

## EXPERIMENTAL

### Materials

Silver nitrate ($AgNO_3$) was obtained from S.D. Fine Chem, Mumbai, India. Zinc sulphate ($ZnSO_4 \times 7H_2O$) and ammonium hydroxide ($NH_4OH$) of analytical grades were purchased from Finar Chemicals Ltd., Ahmadabad, India. NaOH (AR grade) was purchased from Atoma scientific, India. Mercurochrome (97 %) was purchased from HPLC Pvt. Ltd., Mumbai, India. All chemicals were of analytical grade and were used without further purification. Distilled water (Elix 10, millipore) was used for preparing all the aqueous solutions.

### *Methodology for thin film preparation*

In this study Ag:ZnO and pure ZnO thin film prepared by SILAR method. Fig. 1 shows schematic of thin film preparation. In the present work, glass slides and FTO (fluorine doped tin oxide) slides were used as substrate for semiconductor ZnO film preparation. Glass substrate pre-treatment was performed appropriately prior to its utilization. For pre-treatment, glass substrate was dipped in dilute chromic acid (potassium dichromate and sulphuric acid solution) for 10 min and further sonicated for 10 min (in distilled water). It was then washed by acetone-ethanol mixture (1:1 volume ratio acetone to ethanol) for 3 times.

Appropriate number of precursors were dissolved in distilled water to prepare 0.1 M zinc sulphate as well as silver nitrate solution (100 ml) prepared by. The required amount of silver nitrate solution was added drop wise in zinc sulphate solution while continuously stirring. 9 mL of ammonium hydroxide ($NH_4OH$, 13 M) was then added to adjust its pH value to 9.0. pH measurement was carried out in a Systronics pH meter (Model 335). This addition was responsible for forming zincate complex (zinc ammonia complex, $[Zn(NH_3)_4]^{2+}$). However, the thin film obtained at pH = 9 was non-adherent. So, its

pH value was further optimized. On increasing pH to 10 (by the addition of NaOH), film obtained was yet non-adherent and powdery. This is attributed to the fact that film growth rate is highly sensitive to pH of the zincate bath. Consequently, the optimum pH of ammonium zincate bath was found to be 11.7 to obtain adherent and mechanically hard thin film. The solution was further stirred continuously for 30 min to prepare the ultimate zincate bath. 100 mL distilled water was continuously heated at ~96 - 98°C to prepare hot water bath.

The glass substrate was coated by repeated cyclic process. Firstly, substrate was dipped in zincate bath (at ambient condition for 10 s). Further, it was dipped in hot water bath (for 10 s). Consequently, it was dried at 110°C for 15 min and further calcined at 500°C for 2 h. The complete set of the alternate dipping and drying cycle was repeated for 60 times to obtain reasonable thickness. Additionally, highly adherent thin film was also achieved after optimum 60 cycles. Further, pure ZnO thin films were also prepared with similar methodology, except the initial precursor was containing only Zn precursor.

**Mechanism of film growth process**

SILAR method is a two-step method: (i) During zincate bath preparation, ammonium hydroxide addition to zinc sulphate led to zinc ammonia complex ($[Zn(NH_3)_4]^{2+}$) formation. Upon dipping the glass substrate in the zincate bath, the zinc ammonia complex was adsorbed onto the glass substrate.

In the second step, upon further dipping in the hot water bath, the adsorbed zinc ammonia complex was transformed to $Zn(OH)_2$ as follows:

$[Zn(NH_4)]^{+2} + H_2O \rightarrow Zn^{+2} + NH^{+4} + OH^-$ (during the second step) (1)

$Zn^{+2} + OH^- \rightarrow Zn(OH)_2$ (during the second step) (2)

Upon heat treatment, it is further transformed as follows:

$Zn(OH)_2 \rightarrow [Zn^{+2} + 2(O^- + H^+)]^{(solid)}$ (upon heat treatment) (3)

It is further transformed into oxide phase at the higher temperature in the muffle furnace in the presence of air:

$[Zn^{+2} + 2(O^- + H^+)]^{(solid)} + O_2^{gas} \leftrightarrow [ZnO]^{solid} + H_2O + O_2^{gas}$ (upon further calcination) (4)

**DSSC preparation and evaluation**

Fig. 2 shows schematic of DSSC fabricated using both pure ZnO and Ag:ZnO films as photoanode. The films were immersed into 0.5 mM mercurochrome dye in ethanol for 3h at room temperature. The platinum coated electrode was prepared by spin coating process. Redox $I^-/I^{3-}$ electrolyte containing 0.5 M LiI and 0.05 M $I_2$ in acetonitrile was used in between two assembled electrodes, as shown in our previous work. The photovoltaic properties of the solar cells were measured using the solar simulator under AM 1.5G (100 mW $cm^{-2}$, Newport, USA) and 2400 Source Meter (Keithley, USA).

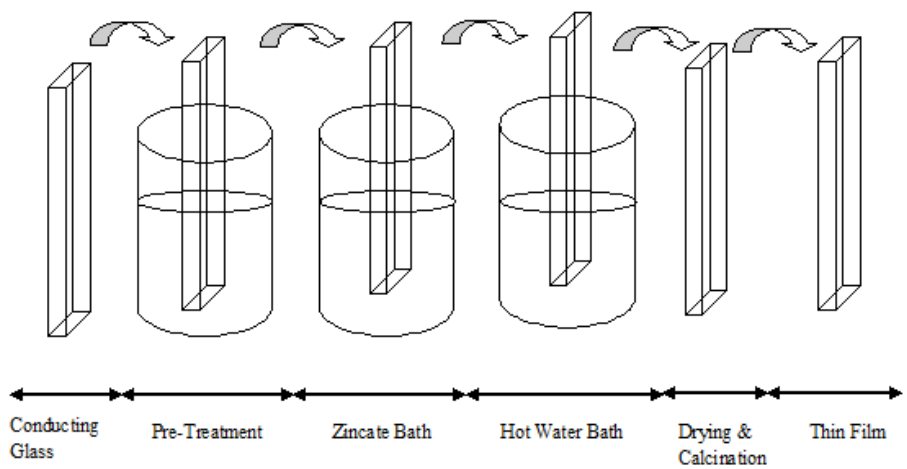


Fig. 1. Schematic of methodology for thin film preparation.

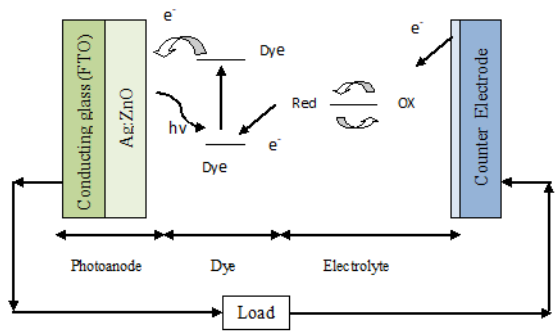


Fig. 2. Schematic of synthesized dye sensitized solar cell (DSSC) with photoanode and counter electrode.

### Characterization of thin film

The optical properties were found by UV-visible spectroscopy (DR 5000 HACH). The band gap of the films was calculated by Tauc's relationship. The doping percentages leading to the maximum reduction of the band gap was optimum. Optimum Ag:ZnO was further investigated for changes in the phase structure by X-ray diffraction (Rigaku, Mini Flex model, Japan) using Cu Kα radiation (λ = 1.5406 Å). Moreover, its surface morphology is examined by SEM (JEOL JSM 5610LV). The thickness of the film was also measured by cross sectional SEM and film monitoring device (Mprobe UV-Vis - SR Spectrometer, M/S Semiconsoft, USA). The film thickness was also obtained by gravimetric method. The increase in weight after coating is basically used to calculate the thickness with usage of the area of coating and ZnO density (5.6 gm $cm^{-3}$).

## RESULTS AND DISCUSSION

### UV-Vis spectroscopy

UV-Vis spectroscopy of pure ZnO thin film and Ag:ZnO thin film with various wt. % of Ag dopant is investigated. The optical absorbance of film is investigated, as shown in Fig. 3a. Variation in $\lambda_{max}$ with doping percentages is depicted in Fig. 3b. The absorption peak ($\lambda_{max}$) is observed at 372 nm for pure ZnO thin film,

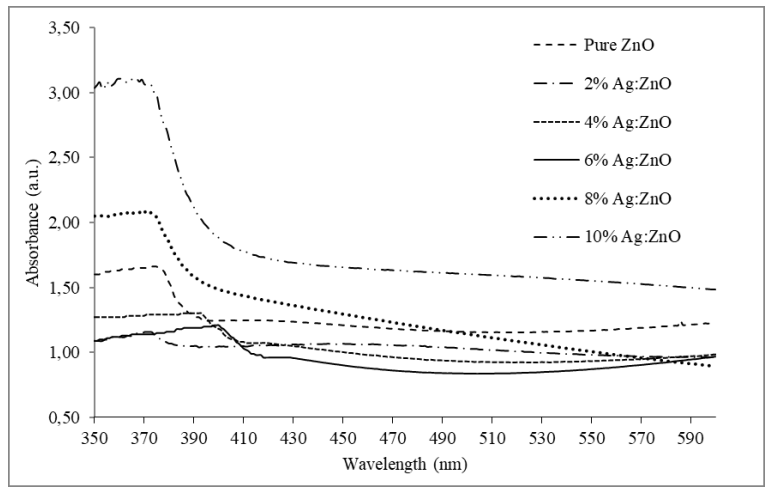


Fig. 3(a). UV-Vis Spectroscopy of pure ZnO thin film and Ag:ZnO thin film with various wt. % of Ag dopant, at 2 %, 4 %, 6 %, 8 %, 10 %.

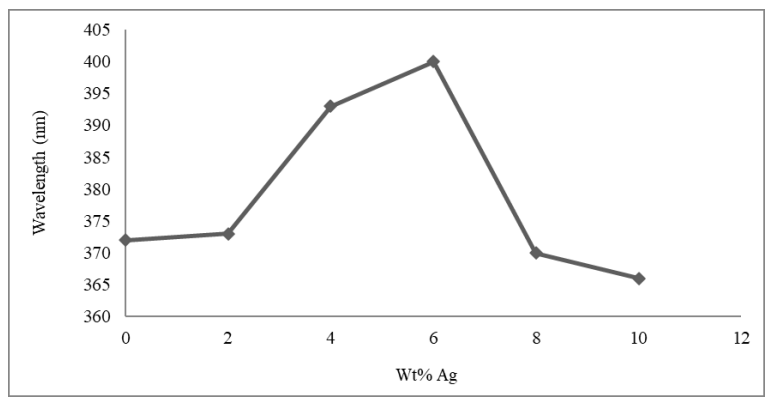


Fig. 3(b). Variation Variation of wavelength (nm) shifted with % Ag doping (2 % - 10 % dopant amount) with ZnO.

which is the characteristic absorption peak of ZnO [4]. Absorbance peak ($\lambda_{max}$) of thin film is observed to give a red shift with the increase in amount of dopant (from 2 % to 6 %). With 6 wt. % Ag, the $\lambda_{max}$ observed is highest (400 nm), which is maximum absorption wavelength among all Ag dopant and pure ZnO thin films. Basically, the red shift is associated with the decrease in band gap more towards visible range. It means film (6 wt. %) can capture visible spectrum at the high extent in comparison with that of the pure ZnO film [24 - 36]. The red shift is attributed to the substitution of zinc atom by Ag [35], and Ag has good photoluminescence in visible range.

However, on further increase in amount of Ag (from 8 % to 10 %), it is observed that $\lambda_{max}$ reduced from 400 to 366 nm. This is attributed to excess doping, because it leads to more oxygen vacancies and high electron concentration [31]. Thus, it is concluded that optimum doping is 6 % Ag:ZnO.

**Bang gap calculation with Tauc's relationship measurement**

The optical band gap is calculated with Tauc's relationship as follows [4].

$$\alpha h\upsilon = A(h\upsilon - Eg)\text{^}n \quad (5)$$

where, α is absorption coefficient, hυ is the photon energy, Eg is the band gap, n = 1/2 for direct transitions, A is constant, h is Plank's constant ($6.626\times10^{-34}$ J.s) and is C/λ. C is the velocity of light (C = $3\times10^{8}$ m $s^{-1}$). α is calculated using the equation,

$$\propto = lnT \quad (6)$$

where, T is transmittance. It is given by following the equation:

$$T = \frac{10^{(2-A)}}{100} \quad (7)$$

Using this relationship, $(\alpha h\upsilon)^2$ vs. hυ (eV), Tauc's plot is plotted as shown in Fig. 4. $E_g$ (Direct band gap energy) is subsequently obtained from this plot. Consequently, obtained Eg vs. Ag amount (wt. %) is depicted in Fig. 5.

Fig. 5 shows that on varying Ag amount (from 2 to 10 %), maximum reduction in band gap is obtained at 6 wt. % (2.7 eV). The initial decrease in band gap

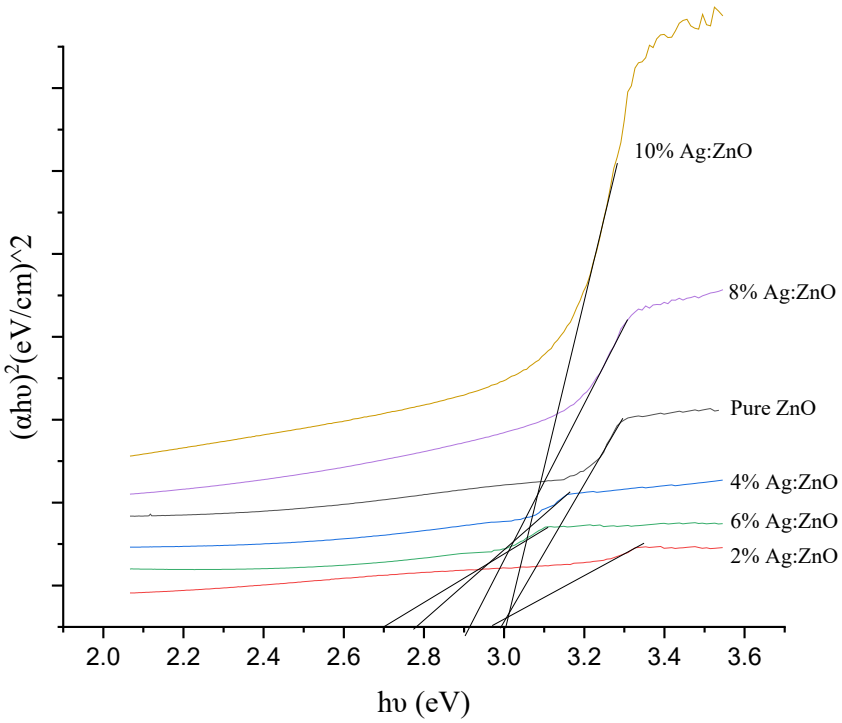


Fig. 4. Tauc's plot for pure ZnO and various wt. % of Ag:ZnO (2 %, 4 %, 6 % ,8 %,10 %).

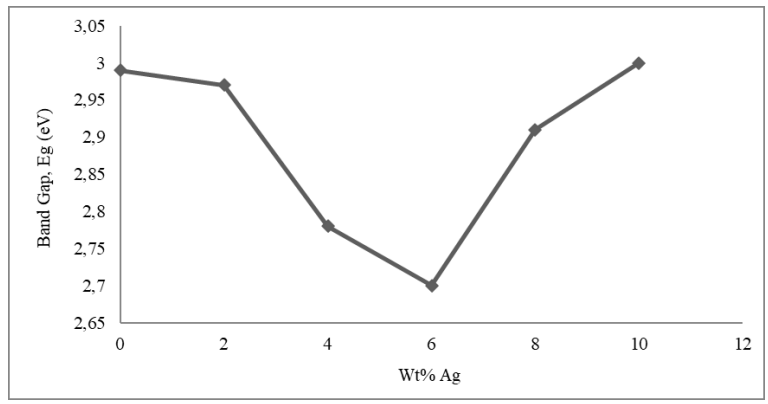


Fig. 5. Variation of band gap (eV) with variation in wt. % of Ag doping on ZnO.

up to 6 wt. % Ag doping can be attributed to the substitution of $Ag^{+}$ ions into the $Zn^{2+}$ lattice sites, which introduces defect levels and modifies the electronic structure. However, the subsequent increase in band gap beyond 6 wt. % may be due to the onset of Ag ion clustering or formation of secondary Ag-rich phases, which reduces the effective incorporation of Ag into the ZnO lattice. Such clustering behaviour at higher doping levels is consistent and may explain the non-monotonic band gap variation observed in this study. The decreased band gap may be attributed to existence of Ag impurities in zinc, which leads to formation of new recombination centers with lower energy state [36]. After Ag amount addition of 6 wt. % Ag, the band gap widens because, the substitution of $Zn^{+}$ by $Ag^{+}$ increases electron concentration and electron vacancy due to electronegativity and ionic radius difference (between Zn and Ag) may be also responsible for the above decrease. Basically, ionic radius difference and electronegativity increase carrier density, which leads to lifting of Fermi level towards the conduction band, and consequently band gap widen [31]. Thus, it is confirmed that optimum doping wt. % is 6 %. Consequently, optimum Ag:ZnO was further investigated by X-ray diffraction (for changes in the phase structure) and SEM (for surface morphology).

**X-Ray diffraction (XRD) of optimum Ag:ZnO film**

XRD pattern of optimum Ag:ZnO film is recorded and compared with pure ZnO film XRD pattern (Fig. 6). The strongest detected peaks are at 2θ values of 31.80°, 34.42°, 36.22°, 47.51°, 56.62°, 62.86°, 66.42°, 68.0°, and 69.12° corresponding to the following lattice planes: (100), (002), (101), (102), (110), (103), (200), (112) and (201) respectively (JCPDS card No. 36-1451). This depicts the presence of crystalline ZnO with the hexagonal wurtzite structure, in agreement with the literature [33]. As observed from Fig. 6, 6 % Ag:ZnO thin film does not show the presence of dopant Ag phase peak at 38.44° and 46.30° (JCPDS 04-0783). This may be because low content of Ag [17]. Further, no characteristic peak of any other impurity phase (Zn, $Zn(OH)_2$, S) is observed. It depicts the proper doping of Ag on ZnO.

Debye-Scherer's Eq. (8) is used to calculate crystal size:

$$D(2\theta) = K\lambda/LCos\theta \quad (8)$$

where, D is crystal size, is the wavelength of X-ray (nm), L is full width at half maximum (FWHM), and K is constant of proportionality (which depends on how the width is determined, the shape of the crystal and size distribution). Generally, K = 0.94 (for spherical particles with approximate cubic symmetry), which is used in the present work.

The crystal size of 6 % Ag:ZnO thin film is calculated to be 55.8 nm. However, crystal size of pure ZnO thin film is calculated to be 120.9 nm. The result shows decrease in crystal size upon doping. The crystal size reduced due to increase in 2θ value with increase in FWHM value (FWHM increased from 0.12 nm to 0.26 nm upon doping) [31]. This result may be attributed to Zener pining effect [32, 37].

XRD pattern depicts the minor shift of the peak (100), which is due to $Zn^{2+}$ replacement by $Ag^{+}$.

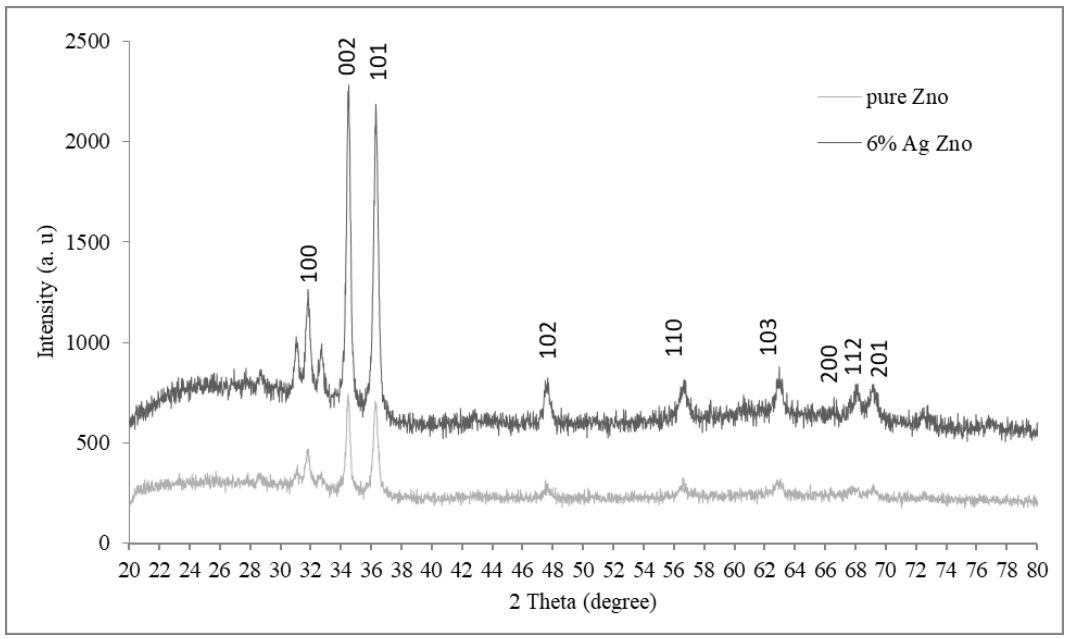


Fig. 6. XRD pattern of pure ZnO and optimum (6 wt. %) Ag:ZnO thin film.

Basically, the ionic radius of Ag is larger (0.126 nm) than that of Zn (0.074 nm) [33, 34]. Upon doping, the increase in intensity of lattice planes at (100), (101), (002) is also observed (Fig. 6). This is attributed to heterogeneous nucleation facilitated in the presence of $Ag^{+}$ ions [33, 34].

**Scanning electron microscopy (SEM) of optimum Ag:ZnO thin film**

The morphology of optimum Ag:ZnO was further investigated by SEM (scanning electron microscope). Fig. 7 depicts the SEM image of 6 % Ag:ZnO. For comparison, SEM image of pure ZnO film is also shown in Fig. 8. SEM analysis reveals that the pure ZnO film exhibits a porous and polycrystalline morphology. The surface is composed of uniformly distributed spherical particles, with sizes ranging from 480 to 600 nm. These particles are likely aggregates of smaller crystallites. XRD analysis confirms the polycrystalline nature of the film. Although no cracks are observed, the presence of few holes is detected, which indicates porosity. Similar morphology is also observed by Mondal et al. [16]. It is clearly observed that doped film is relatively more compact and uniform than that of pure ZnO film (Fig. 7). The denseness of film is increased upon doping. Further, it is also observed that Ag appears to be brighter than ZnO and spherical in shape.

**Film thickness measurement of optimum Ag:ZnO thin film**

***Thickness measurement of optimum Ag:ZnO film by thickness monitor***

The thickness of the film was measured by film monitoring device (Mprobe UV-Vis -SR Spectrometer, M/S Semiconsoft, USA) based on spectroscopic reflectometry. The instrument records the reflectance spectrum over a broad wavelength range (typically 200 - 1100 nm), and the film thickness is determined by fitting the measured spectrum to a theoretical model using known optical constants of the film and substrate. The film thickness obtained for optimum Ag:ZnO film was observed to be 2.82 μm. The film thickness obtained for pure ZnO thin film is also approximately same (2.8 μm).

***Thickness measurement by cross sectional SEM***

Cross sectional SEM is also performed and consequently used for film thickness measurement. Fig. 9 depicts the cross-sectional SEM images of optimum Ag:ZnO film. From Fig. 9, the film thickness can be obtained by calculating the difference between thickness of substrate with coating (14.8 μm) and without coating (12 μm). From Fig. 9, it is clearly observed that the thickness of ZnO thin film is approximately 14.8 μm - 12 μm = 2.8 μm. The identical thickness is obtained for pure ZnO thin film (2.78 μm).

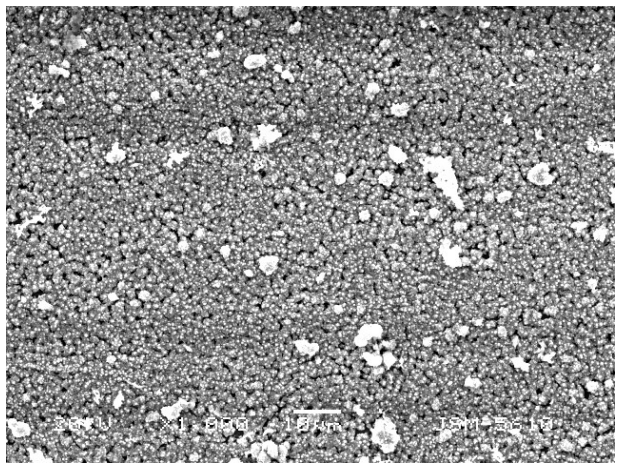

Fig. 7. SEM images of optimum (6 wt. %) Ag:ZnO thin film.

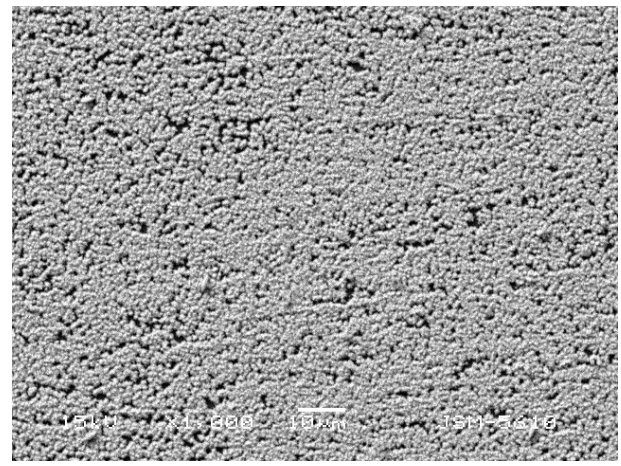

Fig. 8. SEM images of pure ZnO thin film prepared.

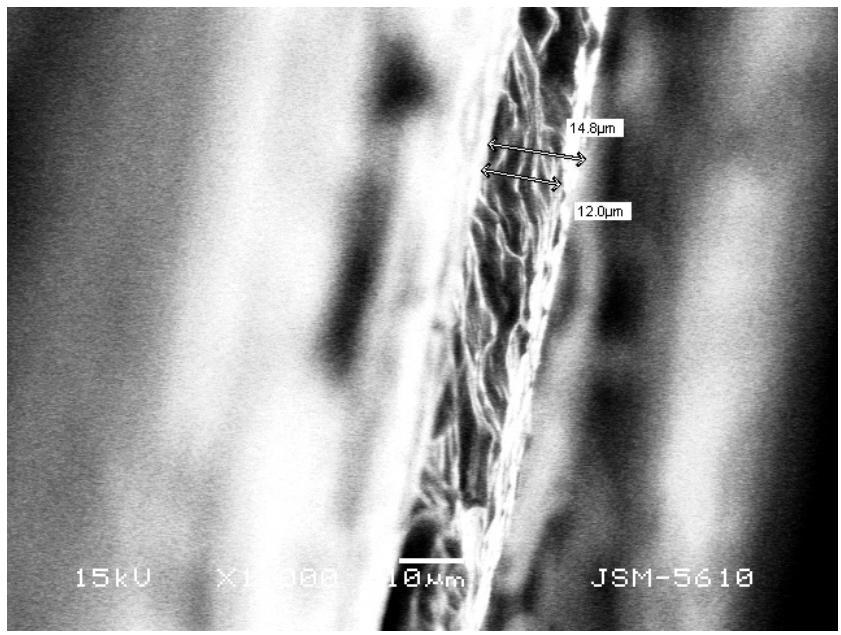


Fig. 9. Cross sectional SEM images of optimum (6 wt. %) Ag:ZnO thin film.

***Thickness measurement by gravimetric method***

The film thickness is also calculated by gravimetric method. It involves thickness (d) calculation with change in weight of the substrate (upon film deposition).

$$d = \frac{w_2 - w_1}{A\rho} * 10^4\ \mu m \quad (9)$$

where, A is the area of film deposition ($cm^2$), and ρ is the theoretical density of ZnO (5.6 gm $cm^{-3}$), $w_1$ and $w_2$ and are weights of substrates (gm), before and after the film deposition, respectively [30]. The film thickness increases linearly with increase in the number of dipping cycles. In the present work, the thickness of the film is found to be 2.9 µm (with 60 times dipping). The thickness is approximately identical to that obtained with thickness monitor and cross-sectional SEM. There is a negligible difference observed attributed to the additional weight (coated on edges of glass substrate) considered in the gravimetric method.

**DSSC performance evaluation of optimum Ag:ZnO thin film**

DSSC performance is evaluated for optimum (6 %) Ag:ZnO film. For comparison, pure ZnO film is also evaluated. Dye used for sensitization was an economic

dye (mercurochrome). Fig. 10 depicts photocurrent-voltage characteristics of DSSC under AM 1.5G illumination. Current density, $J_{sc}$ (mA $cm^{-2}$), fill factor, FF (%), $V_{oc}$ (V), and overall efficiency, η (%) are represented in Table 1. The overall DSSC efficiency (η) is calculated using Eq. (10) [38].

$$\eta\,(\%) = \frac{Isc\ x\ Voc}{Pin}\ x\ FF \qquad (10)$$

where, $P_{in}$ is the incident light power.

Fill factor (FF) was calculated according to the Eq. (11) [38].

$$FF(\%) = \frac{Pmax}{Isc\ x\ Voc}\ x\ 100 \qquad (11)$$

where, $V_{oc}$ and $I_{sc}$ are open circuit voltage and short circuit current. $P_{max}$ is the maximum power delivery point.

Ag doping in ZnO leads to enhanced current density as well as conversion efficiency. There is a reasonable increase of 50 % in conversion efficiency. In addition, generally used dyes (N719 and N3) are costly. However, the low-cost dye (mercurochrome) used in the present study also led to reasonable increase in conversion efficiency. The increase is comparable to that reported with costly dyes [39]. Although mercurochrome is a low-cost dye alternative for dye-sensitized solar cell (DSSC) sensitization, its mercury content raises potential health and environmental concerns. In the present study, mercurochrome was employed in minimal concentration (0.5 mM per DSSC). The dye was applied to the photoanode and subsequently enclosed within the sealed DSSC structure by overlaying with a conducting cathode glass, thereby preventing any direct exposure to the external environment. The primary objective of utilizing mercurochrome was to evaluate its optical absorption characteristics and electron transfer capabilities, with a focus on exploring its feasibility for low-cost DSSC fabrication.

## CONCLUSIONS

Ag:ZnO thin films are successfully synthesized by the SILAR method. It is a simple, low-cost method, which can give large scale production. The maximum red shift in absorbance (by UV-Vis spectroscopy) revealed optimum amount of Ag:ZnO to be 6 wt. %. Additionally, optimum amount (6 wt. %) also led to the maximum reduction of the band gap (2.99 eV to 2.7 eV). The polycrystalline nature of optimum films is confirmed appropriately (by XRD characterization).

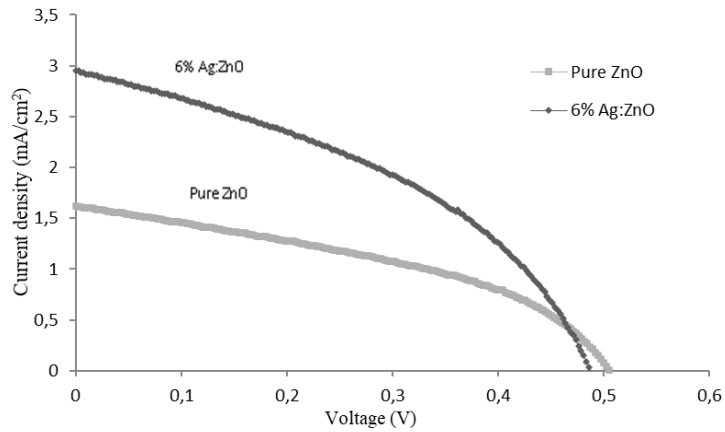


Fig. 10. Photocurrent- voltage characteristics of optimum (6 wt. %) Ag:ZnO thin film and pure ZnO films.

Table 1. DSSC parameters of pure ZnO and optimum (6 wt. %) Ag:ZnO thin films under AM 1.5G illumination.

| Photoanode | $V_{oc,}$ V | Current density, $J_{sc}$, mA $cm^{-2}$ | Fill Factor, FF, % | Efficiency, η, % |
|---|---|---|---|---|
| Pure ZnO | 0.50 | 1.77 | 46.39 | 0.42 |
| 6 % Ag:ZnO | 0.49 | 2.95 | 43.98 | 0.63 |

The film thickness estimated by thickness monitor, cross sectional SEM and gravimetric method are almost identical (2.8 μm). DSSC performance evaluated with optimum Ag:ZnO clearly reveals improvement in overall conversion efficiency by 50 %, as compared to pure ZnO. Further exploration for better improvement is still essential. Nevertheless, these results are quite encouraging due to the use of a low-cost dye, low-cost material (ZnO), and a low-cost film preparation method (SILAR).

***Acknowledgements***

*The authors acknowledge the Sophisticated Analytical Instrument Facility (SAIF), Indian Institute of Technology, Bombay, Central facility, Indian Institute of Technology, Gandhinagar, Sophisticated instrumentation center for applied research and testing, Anand and Sardar Vallabhbhai National Institute of Technology, Surat, Gujarat India, for rendering analytical services for this work.*

*This research did not receive any specific grant from funding agencies in the public, commercial or not-for-profit sectors.*

***Authors' contributions***

*M.K.L.: Formal analysis of data, conducting research, Data curation and analysis, writing original draft of manuscript. J.V.G.: Writing - Conceptualization and formulation of research objectives and aims, Development of Methodology, Project administration, planning and execution, Data analysis and assessment, Visualization, Provision of resources, Review & editing of manuscript, Supervision and mentorship.*

**REFERENCES**

1. A. Umar, Growth of Comb-like ZnO Nanostructures for Dye-sensitized Solar Cells Applications, Nanoscale Res. Lett., 4, 2009, 1004-1008. https://doi.org/10.1007/s11671-009-9353-3
2. T.H. Tsai, S.C. Chiou, S.M. Chen, K.C. Lin, Enhanced Photoelectrochemical Performance of Dye-Sensitized Solar Cells base on Iodine-PEDOT Composited Film, Int. J. Electrochem. Sci., 6, 2011, 3938-3950. https://doi.org/10.1016/s1452-3981(23)18301-5
3. A.K.K. Kyaw, X.W. Sun, J.L. Zhao, J.X. Wang, D.W. Zhao, X.F. Wei, T. Wu, Top-illuminated dye-sensitized solar cells with a room-temperature-processed ZnO photoanode on metal substrates and a Pt-coated Ga-doped ZnO counter electrode, J. Phys. D: Appl. Phys., 44, 2011, 045102. https://doi.org/10.1088/0022-3727/44/4/045102
4. A. Raidou, M. Aggour, A. Qachaou, L. Laanab, M. Fahoume, Effect of substrate on ZnO thin films grown by SILAR method, MJ. Condensed Matter, 12, 2010, 125. https://doi.org/10.1109/irsec.2014.7059829
5. F. Claeyssens, C.L. Freeman, N.L. Allan, Y. Sun, M.N. Ashfold, J.H. Harding, Growth of ZnO thin films-experiment and theory, J. Mater. Chem., 15, 2005, 139-148. https://doi.org/10.1039/b414111c
6. P. Mitra, S. Mondal, Structural and Morphological Characterization of ZnO thin Films Synthesized by SILAR, Progress Theoretical Appl. Phys., 1, 2013, 17-31. https://doi.org/10.1088/1757-899X/571/1/012111.
7. A. Martın, J.P. Espinos, A. Justo, J.P. Holgado, F. Yubero, A.R. González-Elipe, Preparation of transparent and conductive Al-doped ZnO thin films by ECR plasma enhanced CVD, Surf. Coat. Tech., 151, 2002, 289-293. https://doi.org/10.1016/s0257-8972(01)01609-7
8. K.H. Kim, K. Utashiro, Z. Jin, Y. Abe, M. Kawamura, Structural Properties of Zinc Oxide Nanorods Grown on Al-Doped Zinc Oxide Seed Layer and Their Applications in Dye-Sensitized Solar Cells, Materials, 7, 2014, 2522-2533. https://doi.org/10.3390/ma7042522
9. L. Wang, Y. Kang, X. Liu, S. Zhang, W. Huang, S. Wang, ZnO nanorod gas sensor for ethanol detection, Sensors and Actuators B: Chemical, 162, 2012, 237-243. https://doi.org/10.1016/j.snb.2011.12.073
10. S.H. Baek, B.Y. Noh, I.K. Park, J.H. Kim, Fabrication and characterization of silicon wire solar cells having ZnO nanorod antireflection coating on Al-doped ZnO seed layer, Nanoscale Res. Lett., 7, 2012, 29. https://doi.org/10.1186/1556-276x-7-29
11. S. Choudhary, S. Upadhyay, P. Kumar, N. Singh, V.R. Satsangi, R. Shrivastav, S. Dass, Nanostructured bilayered thin films in photoelectrochemical water splitting-A review, Int. J. Hydrogen Energy, 37,

2012, 18713-18730. https://doi.org/10.1016/j.ijhydene.2012.10.028

12. S. Ilican, Y. Caglar, M. Caglar, Structural, morphological and optical properties of $CuAlS_2$ films deposited by spray pyrolysis method, J. Optoelectron Adv. Mater., 281, 2008, 1615-1624. https://doi.org/10.1016/j.optcom.2007.11.031
13. S. Mondal, K.P. Kanta, P. Mitra, Preparation of Al-doped ZnO (AZO) Thin Film by SILAR, J. Phys. Sci., 12,2008,221-229. http://inet.vidyasagar.ac.in:8080/jspui/handle/123456789/764
14. S.J. Pearton, D.P. Norton, M.P. Mil, A.F. Hebard, J.M. Zavada, W.M. Chen, I.A. Buyanova, ZnO Doped With Transition Metal Ions, IEEE Trans. Electron., 54, 2007, 1040-1048. https://doi.org/10.1109/ted.2007.894371
15. S. Ilican, Y. Caglar, M. Caglar, B. Demirci, Structural, morphological and optical properties of $CuAlS_2$ films deposited by spray pyrolysis method, J. Optoelectron. Adv. Mater., 281, 2008, 1615-1624. https://doi.org/10.1016/j.optcom.2007.11.031
16. S. Mondal, P. Mitra, Preparation of Ni doped ZnO thin films by SILAR and their characterization, Indian J. Phy., 87, 2013, 125-131. https://doi.org/10.1007/s12648-012-0198-8
17. C. Karunakaran, V. Rajeswari, P, Gomathisankar, Enhanced photocatalytic and antibacterial activities of sol-gel synthesized ZnO and Ag-ZnO, Mater. Sci. Semicond. Process, 14, 2011, 133-138. https://doi.org/10.1016/j.mssp.2011.01.017
18. A.S. Kuznetsov, Y.G. Lu, S. Turner, M.V. Shestakov, V.K. Tikhomirov, D. Kirilenko, J. Verbeeck, A.N. Baranov, V.V. Moshchalkov, Preparation, structural and optical characterization of nanocrystalline ZnO doped with luminescent Ag-nanoclusters, Opt. mater. Express, 2, 2012, 723. https://doi.org/10.1364/ome.2.000723
19. M. Lanjewar, J.V. Gohel, Enhanced performance of Ag-doped ZnO and pure ZnO thin films DSSCs prepared by sol-gel spin coating, Inorg. Nano-Metal Chem., 47, 2017, 1090-1096. https://doi.org/10.1080/24701556.2016.1241275
20. Q. Zhang, G. Cao, Nanostructured photoelectrodes for dye-sensitized solar cells, Nano Today, 6, 2011, 91-109. https://doi.org/10.1016/j.nantod.2010.12.007
21. C. Karunakaran, V. Rajeswari, P. Gomathisankar, Enhanced photocatalytic and antibacterial activities of sol-gel synthesized ZnO and Ag-ZnO, Mater. Sci. Semicond. Process, 14, 2011, 133-138. https://doi.org/10.1016/j.mssp.2011.01.017
22. R. Jayakrishnan, K. Mohanachandran, R. Sreekumar, C. Sudha Kartha, K.P. Vijayakumar, ZnO thin Films with blue emission grown using chemical spray pyrolysis, Mater. Sci. Semicond. Process, 16, 2012, 326-331. https://doi.org/10.1016/j.mssp.2012.10.003
23. H. Kim, J.Y. Moon, H.S. Lee, Growth of ZnO nanorods on various substrates by electrodeposition, Electron. Mater. Lett., 5, 2009, 135-138. https://doi.org/10.3365/eml.2009.09.135
24. J.N. Solanki, Z.V.P. Murthy, Highly monodisperse and sub-nano silver particles synthesis via microemulsion technique, Colloids. Surf. A., 359, 2010, 31-38. https://doi.org/10.1016/j.colsurfa.2010.01.058
25. P.S. Mishra, J.N. Solanki, Z.V.P. Murthy, $TiO_2$ nanoparticles synthesis for application in proton exchange membranes, Cryst. Res. Technol., 48, 2013, 969-976. https://doi.org/10.1002/crat.201300179
26. J.N. Solanki, Z.V.P. Murthy, Preparation of Silver Nanofluids with High Electrical Conductivity, J. Dispersion. Sci. Technol., 32, 2011, 724-730. https://doi.org/10.1080/01932691.2010.480863
27. J.N. Solanki, R. Sengupta, Z.V.P. Murthy, Synthesis of copper sulphide and copper nanoparticles with microemulsion method, Solid. State. Sci., 12, 2010, 1560-1566. https://doi.org/10.1016/j.solidstatesciences.2010.06.021
28. M. Lanjewar, J.V. Gohel, Highly enhanced solar conversion efficiency of novel layer-by-layer PbS:Hg and CdS quantum dots-sensitized ZnO thin films prepared by sol-gel spin coating, Bull. Mater. Sci., 41, 2018, 151. https://doi.org/10.1007/s12034-018-1664-5
29. J.N. Solanki, Z.V.P. Murthy, Reduction of 4-Chlorophenol by Mg and Mg-Ag Bimetallic Nanocatalysts, Ind. Eng. Chem. Res., 50, 2011, 14211-14216. https://doi.org/10.1021/ie2022338
30. J.N. Solanki, Z.V.P. Murthy, Controlled Size Silver Nanoparticles Synthesis with Water-in-Oil Microemulsion Method: A Topical Review, Ind. Eng. Chem. Res., 50, 2011, 12311-12323. https://

doi.org/10.1021/ie201649x

31. A. Agrawal, T.A. Dar, P. Sen, Anomalous band bowing in pulsed laser deposited $Mg_xZn_{1-x}O$ films, J. Nano-Electron. Phys., 384, 2013, 9-12. https://doi.org/10.1016/j.jcrysgro.2013.08.036
32. K. Thongsuriwong, P. Amornpitoksuk, S. Suwanboon, Photocatalytic and antibacterial activities of Ag-doped ZnO thin films prepared by a sol-gel dip-coating method, J. Sol-Gel Sci. Technol., 62, 2012, 304-312. https://doi.org/10.1007/s10971-012-2725-7
33. O. Lupan, L. Chow, L.K. Ono, B.R. Cuenya, G. Chai, H. Khallaf, A. Schulte, Synthesis and Characterization of Ag- or Sb-Doped ZnO Nanorods by a Facile Hydrothermal Route, J. Phys. Chem. C., 114, 2010, 12401-12408. https://doi.org/10.1021/jp910263n
34. M. Yousefi, M. Amiri, R. Azimirad, A.Z. Moshfegh, Enhanced photoelectrochemical activity of Ce doped ZnO nanocomposite thin films under visible light, J. Electroanal. Chem., 661, 2011, 106-112. https://doi.org/10.1016/j.jelechem.2011.07.022
35. J.S. Tawale, A. Kumar, A. Mohan, A.K. Srivastava, Influence of silver and graphite on zinc oxide nanostructures for optical application, Opt. Mater., 35, 2013, 1335-1341. https://doi.org/10.1016/j.optmat.2013.01.034
36. M.S. Kim, K.G. Yim, S. Kim, G. Nam, D.Y. Lee, J.S. Kim, J.Y. Leem, Growth and Characterization of Indium-Doped Zinc Oxide Thin Films Prepared by Sol-Gel Method. Acta Phys Pol A. 121, 2012, 217-220. https://doi.org/10.12693/aphyspola.121.217
37. S. Suwanboon, P. Amornpitoksuk, A. Sukolra, Dependence of optical properties on doping metal, crystallite size and defect concentration of M-doped ZnO nanopowders (M = Al, Mg, Ti), Ceramics International, 37, 2011, 1359-1365. https://doi.org/10.1016/j.ceramint.2010.12.010
38. S.D. Satpute, J.S. Jagtap,1 P.K. Bhujbal, S.M. Sonar, P.K. Baviskar, S.R. Jadker, H.M. Pathan, Mercurochrome sensitized ZnO/$In_2O_3$ photoanode for dye sensitized solar cell, ES Energy Environ., 9, 2020, 89-94. https://dx.doi.org/10.30919/esee8c720
39. E.M. Jin, X.G. Zhao, J.Y. Park, H.B. Gu, Enhancement of the photoelectric performance of dye-sensitized solar cells using Ag-doped $TiO_2$ nanofibers in a $TiO_2$ film as electrode, Nanoscale Res. Let., 7, 2012, 97. https://doi.org/10.1186/1556-276x-7-97